www.ietdl.org

Published in IET Renewable Power Generation
Received on 21st July 2013
Revised on 8th April 2014
Accepted on 11th April 2014
doi: 10.1049/iet-rpg.2013.0242

Special Section: 9th Photovoltaic Science, Application and Technology Conference 2013

ISSN 1752-1416

Distributed electrical network modelling approach for spatially resolved characterisation of photovoltaic modules

Xiaofeng Wu[1], Martin Bliss[1], Archana Sinha[2], Tom Betts[1], Rajesh Gupta[2], Ralph Gottschalg[1]

[1]Centre for Renewable Energy Systems Technology (CREST), Loughborough University, Loughborough LE11 3TU, UK
[2]Department of Energy Science and Engineering, Indian Institute of Technology Bombay, Powai, Mumbai 400076, India
E-mail: x.wu2@lboro.ac.uk

Abstract: Distributed electrical modelling and simulation plays an important role in investigating local operating points and the overall power generation of photovoltaic (PV) modules. A PV module is a three-dimensional device in which inhomogeneities can cause a non-uniform performance and hence, electrical mismatches which consequently reduce the overall power generation. Distributed modelling and simulation can be used to identify local electrical properties and their impacts on the power output. In this study, a flexible, distributed electrical network modelling approach is presented. The proposed approach introduces a hierarchical architecture built up from the diode model-based sub-cell level to the module level. A PV-oriented nodal analysis solver is developed to enable the spatially resolved quantitative analysis of electrical operating points by given local properties including irradiance, temperature, series resistance, shunt resistance and ideality factor. The approach has been verified by PSpice software. The case studies have shown that this modelling and simulation tool can be used to analyse spatially resolved characterisation results and to predict global and distributed operating points under different conditions.

1 Introduction

Modelling of a photovoltaic (PV) module provides an insight into the basic physics of their operation and better understanding of the effects of parameter variation and defects causing the loss of efficiency or power yield. Lumped modelling techniques are widely used for PV module characterisation and simulation, and have been proven effective to evaluate global performance and parameters [1–6]. However, a PV module is a three-dimensional device in which there may be considerable inhomogeneities that can cause spatially non-uniform performance and hence, electrical mismatches which consequently reduce the overall power generation and efficiency. Distributed electrical modelling techniques are developed to investigate local properties and their impacts on the overall power generation. In distributed modelling, a whole module is virtually divided into a certain number of sub-circuit units where the spatial information is accessible. Electrical simulation tools are used to solve the circuit network to obtain local operating points. A number of distributed modelling and simulation techniques have been published and validated [7–17]. Most of them used existing circuit analysis software (e.g. SPICE) to support their processes [7–9, 11–15, 17]. This kind of software is powerful and mature on circuit analysis, however is not naturally equipped with some essential interfaces (such as irradiance, temperature, spectrum etc.) for PV applications and complicated pre-processing seems to be required. Computational expense is also an important issue because for a high-resolution modelling task the scale of the circuit network can be huge, but there are no optimisation mechanisms provided by the above-mentioned software.

In this paper, a distributed electrical network modelling approach is reported as an initial stage of a unified modelling and tool for characterisation of PV modules. The model uses the physical parameters (photocurrent, diode saturation current, diode ideality factor, series resistance and shunt resistance) to describe the behaviour of a PV device. The underlying diode equivalent circuit is the core of the modelling tool, with the interfaces to thermal and optical properties being created. A hierarchical architecture ensures not only the mismatch effects at all levels, but also the computational expense is significantly lower than that of a full finite element model.

The rest of the paper is organised as follows: firstly, the hierarchical module architecture is introduced, followed by an elaboration of the simulation engine of the circuit network. The modelling and simulation approach is then verified by comparing its results with a corresponding PSpice simulation. Discussions are made in terms of application issues including verifying mismatch effects caused by spatial inhomogeneities, as well as the possibility of combining this modelling and simulation approach with spatially resolved mapping or imaging techniques to achieve quantitative electrical characterisations.

2 Methodology

2.1 Hierarchical architecture

A hierarchical architecture is introduced to represent the electrical topology in PV modules. Physically, cells are basic units in a PV module. A module is a collection of cells connected following a specific topological structure to meet the required output specifications. Bishop proposed a six-level hierarchical architecture [16] that divides a module into branches (each of which can be protected by a blocking diode), then blocks (each of which can be bridged by bypass diodes). A block can then be further broken into series sub-blocks in which there are parallel strings. By specifying the number of proximate lower-level units in each level (*nBranch*, *nBlock*, *nSubBlk*, *nString* and *nCell*, respectively), an electrical topology of the module can be precisely described (Fig. 1).

However, the original hierarchical architecture was based on lumped model only. To achieve a certain spatial resolution, it is necessary to introduce an appropriate array of virtual sub-cells for each cell. Consequently, the six-level hierarchical architecture is extended with a seventh, that is, the sub-cell level. Each sub-cell is represented by a diode model whose parameters are linked to its parent cell in terms of the size of the sub-cell array, which is determined by the required resolution. A PV-oriented nodal analysis method is developed to enable the solving of spatially resolved electrical operating points and the overall output of each cell. The current–voltage (I–V) characteristic of a cell can be obtained by solving a series of operating points. The I–V curves of cells are then used to derive the characteristics of the higher levels by means of interpolation following a bottom–up manner.

2.2 Model of a virtual sub-cell

A sub-cell is the most elementary unit in the hierarchical structure, as shown in Fig. 2*a*. A single sub-cell contains a PV unit as the core, two resistors radiate to 'west' and 'south', respectively, to represent lateral resistances in the front contact, and other two resistors radiate to 'east' and 'south' to represent lateral resistances in the back contact. The PV unit is a finite area of PV material described by an equivalent diode model [8, 9]. Strictly, the type of the diode

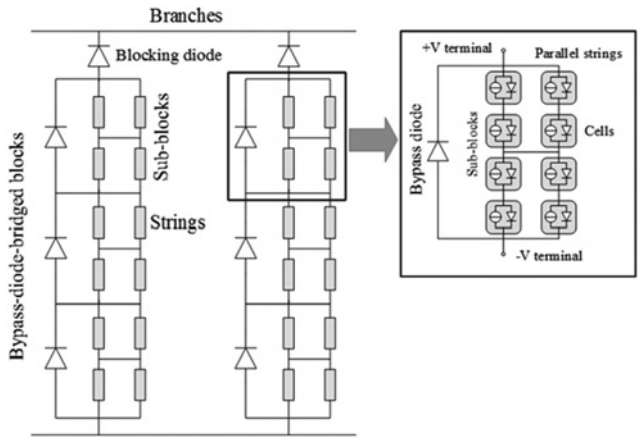

Fig. 1 *Demonstration of a complicated electrical topology in a PV module represented by the six-level hierarchical architecture: in this example, nBranch = 2, nBlock = 3, nSubBlk = 2, nString = 2 and nCell = 2*

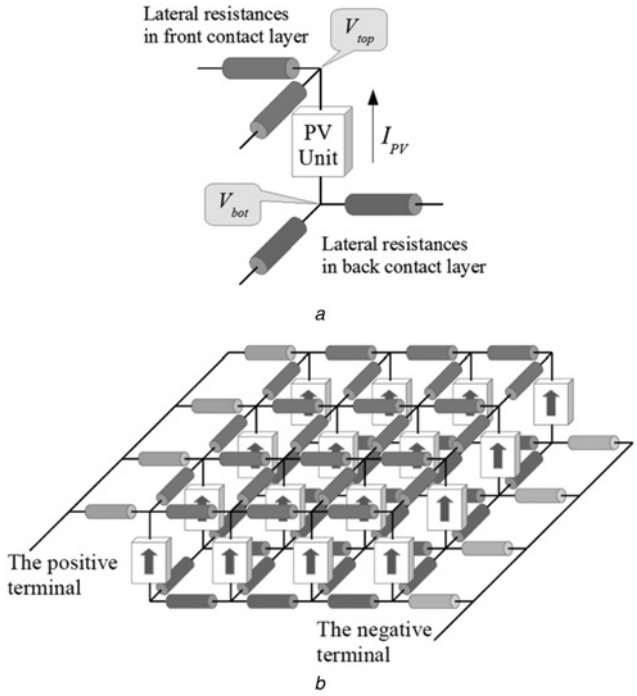

Fig. 2 *Network model in the hierarchical structure*

a Schematic diagram of the model of a virtual sub-cell
b Example of a cell composed by a 4 × 4 array of sub-cells

model is suggested to be material-related. For example, one-diode or double-diode model can be used in the case of crystalline silicon (c-Si) devices whereas Merten's modification is valid for amorphous silicon (a-Si) devices [2]. For simplicity, one-diode model is used in this paper. Lateral resistance is taken into account. It is, especially that in the front contact layer, an important source of series resistance of PV devices. Current flows in most thin-film devices horizontally in the contact layers. Lateral resistances can cause a significant lateral gradient of current and voltage distribution which can be observed from spatially resolved characterisation [e.g. electroluminescence (EL)]. This gradient is a side effect of the relatively high sheet resistance in the transparent conducting oxide with the impact on power production being controlled by creating narrow cells during manufacturing. It remains important to consider lateral resistances especially for spatial characterisation, especially in some special cases where the effects evidently distort the measurements. For c-Si modules, on the other hand, the gradient is not as obvious as it appears in thin-film devices because of the different structure. However, the busbars and fingers can also bring non-uniform current and voltage distribution in the front contact. The lateral resistances in the back contact layer are often seen as being negligible [7, 10, 14]. This assumption works for most small-sized non-bifacial PV cells with metal back contacts which have much higher conductivity compared with the front contact layer. However, in general, the length of the contact layer is much more than its height, so the lateral resistance does inevitably have influences on the lateral current flow and thus the operating points, even if it is sometimes minute. Therefore it is still useful to include the lateral resistances in the back contact.

2.3 Model of a cell

A cell is an assembly of all its children sub-cells in an array whose dimension is determined by a required spatial

doi: 10.1049/iet-rpg.2013.0242

resolution, as shown in Fig. 2*b*. Sub-cells are connected together through lateral resistors. In the lumped modelling approach of Bishop [16], the characteristic of a higher-level unit is obtained by simply combining the *I–V* curves of the lower-level units according to Kirchhoff's circuit law (KCL). However, in this network scenario, the existence of lateral resistances makes the sub-cells no longer two-terminal elements where *I–V* combining can be applied. Instead, a more complicated circuit analysis tool is required.

In this work a modified, that is, PV-oriented, nodal analysis method is developed. Nodal analysis is one of the most popular tools for solving circuit networks and has two major advantages: (i) it is classical and can be relatively easily programmable (it is the computational engine of the widely used circuit simulation tool SPICE [18]), and (ii) its output, that is, the nodal voltages (include V_{top} and V_{bot} of each sub-cell as shown in Fig. 2*a*), can be easily used to derive global and distributed electrical operating points as desired.

The detailed illustration of nodal analysis is beyond the scope of this paper. Briefly, KCL is implemented on each node of the circuit network. For a cell composed by $M \times N$ sub-cells, there are $2MN+2$ nodes in total as each sub-cell has two (top and bottom) nodes and the cell has a positive terminal node and a negative terminal node. Practically, $2MN+1$ nodes are used in nodal analysis because the negative terminal is set as the reference node of the whole cell with a determined electric potential $V_{\text{ref}}=0$. To each node the nodal equation can be formulated as

$$\sum_{b=1}^{\text{No. of branches}} I_b = 0 \tag{1}$$

where I_b represents the current flowing in each circuit branch from/to the node. If the current is flowing into the node, I_b will be a positive value; if the current is flowing out of the node, I_b will be negative.

The $2MN + 1$ nodal equations can be rearranged into a matrix–vector form

$$\boldsymbol{G} \times \boldsymbol{V} = \boldsymbol{I} \tag{2}$$

where $\boldsymbol{V}$ is the unknown vector containing $2MN+1$ nodal voltages, $\boldsymbol{I}$ is the current vector containing all the independent current sources and $\boldsymbol{G}$ is the conductance matrix (or admittance matrix) of the size $(2MN+1)\times(2MN+1)$. All the nodes are numbered by the role-major rule, where the nodes in the front and back contact layers are numbered from 1 to MN and $MN+1$ to $2MN$, respectively, and the positive terminal is numbered as $2MN+1$. Entries in $\boldsymbol{G}$ depict Ohmic interconnections between adjacent nodes. Briefly, an entry G_{ij} represents the additive inverse of the mutual admittance between the ith and jth nodes, whereas a diagonal entry G_{ii} represents the self-admittance of node i.

Take a 3×3 sub-cell array, for example, there are 19 nodes in the nodal equation system, in which there are 9 nodes for both front and back contact layers, numbered as 1–9 and 10–18, respectively. The positive terminal is numbered as 19. A sub-cell, for example, the one at the second row, second column in the array, can have at most four neighbouring sub-cells, as shown in Fig. 3 To formulate the nodal equation system, KCL (1) is applied to each node. I_{eq} and R_{eq} are the effective current source and the effective resistance, respectively, derived from the *I–V* characteristic of the local PV unit in the linearisation stage (will be discussed later). R_{i_j} represents the lateral resistance between the node and a specific neighbouring node. By re-organising the KCL equations, each nodal equation can be expressed as a linear combination of the unknown node voltages on the left-hand side, with the current source on the right. Therefore all the 19 nodal equations can be formatted into the matrix form (5) with a 19×19 conductance matrix $\boldsymbol{G}$ containing all the coefficients (i.e. the admittance) of the voltage factors.

Nodal analysis requires a linear representation of all the circuit elements. Owing to the use of diode model, however, the circuit network of a cell is non-linear. Newton–Raphson method (NR) is an effective numerical method for solving non-linear equation systems: for a given set of operating condition, NR approximates the solution of a non-linear system through a set of iterative sequences in each of which the non-linear system is updated by the most recent estimation and linearised. Therefore the non-linear network is turned into a sequence of linear networks which can be relatively easily solved. The difference of estimations from every two successive iterative sequences will be checked and the whole procedure will be repeated until the difference value satisfies the tolerance of a pre-defined convergence criterion [18]. This procedure is illustrated in Fig. 4. If this solving process is repeated with a certain current (or voltage) range and a specified step width, the *I–V* curve of the cell can be obtained as the result.

In standard non-linear nodal analysis, each non-linear device is linearised individually. For example, in a one-diode model as shown in Fig. 5*a*, the diode is the only non-linear element. It can, at a specified operating point, be approximated as an equivalent linear conductance and a current source connected in parallel [18]. In this PV-oriented approach, the PV unit is considered as an entire entity to which the linearisation is applied. Fig. 5*b* graphically demonstrates this procedure. For a given operating voltage V_x on the curve, the tangent line is used for linearisation during each iterative sequence of NR. The tangent line intersects the current axis at I_{eq} with the slope G_{eq} as

$$I_{\text{eq}} = I_x - G_{\text{eq}} V_x \tag{3}$$

$$G_{\text{eq}} = \frac{\mathrm{d}I}{\mathrm{d}V}\Big|V_x = \frac{\dfrac{I_0 q}{nkT}\exp\left[\dfrac{q(V-I_xR_{\text{s}})}{nkT}\right]+\dfrac{1}{R_{\text{sh}}}}{1+\dfrac{I_0 qR_{\text{s}}}{nkT}\left[\dfrac{q(V-I_xR_{\text{s}})}{nkT}\right]+\dfrac{R_{\text{s}}}{R_{\text{sh}}}} \tag{4}$$

where I_x is obtained by solving the diode model using an internal loop of NR method.

$$I_x = -I_{\text{ph}} + I_0\left\{\exp\left[\frac{q(V_x - I_xR_{\text{s}})}{nkT}\right]-1\right\}+\frac{V_x - I_xR_{\text{s}}}{R_{\text{sh}}} \tag{5}$$

As a consequence, the full diode equivalent circuit is linearised and electrically represented as an equivalent linear conductance (G_{eq}) and a current source (I_{eq}), as shown in Fig. 5*c*. By applying the PV-oriented approach, each linearised PV unit is further simplified by reducing three elements and one node compared with the standard linearisation procedure.

The linearised nodal system described in (2) is solved by a direct method, that is, Gaussian elimination with back substitution. Direct methods are normally stable when

doi: 10.1049/iet-rpg.2013.0242

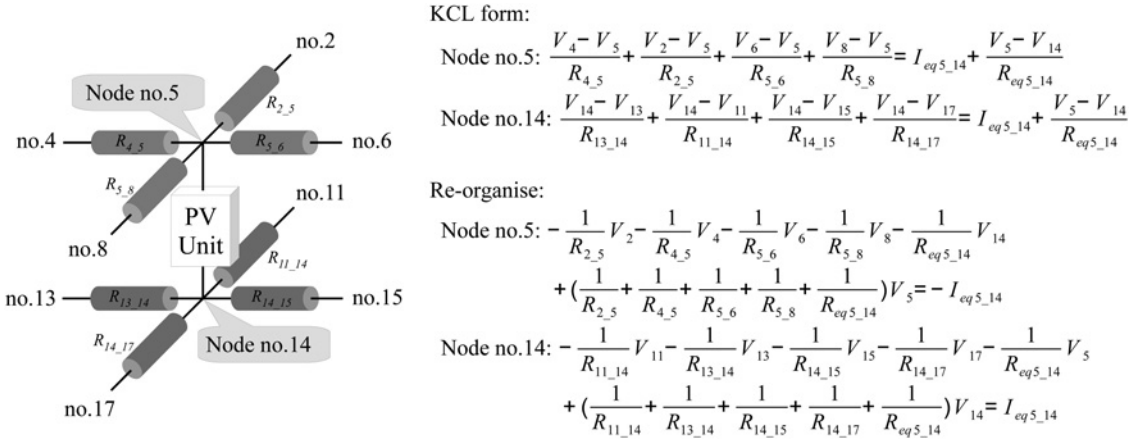

Fig. 3 *Schematic diagram of the sub-cell at the second row, second column in a 3 × 3 sub-cell array with lateral resistances*

The nodal equations of the two nodes are presented

solving well-conditioned linear systems [18]. Since the coefficient matrix $\boldsymbol{G}$ for the circuit network is normally non-singular, there is always a unique solution produced for the linear equation system in each iterative sequence of the NR solver. In addition, a partial pivoting process is introduced to Gaussian elimination to prevent ill-conditioning problems. There are two main problems that could be able to cause the NR to fail: (i) numerical overflow; (ii) non-convergence (e.g. oscillation) [18]. The standard NR algorithm does not provide any mechanism to prevent these two issues to happen, but practically no such unexpected cases have been observed yet.

2.4 Model of a module

A module is the top-most level of the hierarchical tree of the model. Characteristics of all the levels above the cell level are obtained following an identical approach, that is, *I–V* combining. This is done in a bottom–up manner in which all the proximate lower-level units should have obtained their *I–V* curves before their higher-level parents have. In non-ideal cases where inhomogeneities exist, the current and voltage range of each unit is very likely to be different from its neighbours in the same level. Moreover, the units from different levels combine the *I–V* curves along different axes depending on the connection style (in series or in parallel). It is therefore of prime importance to have all the lower-level *I–V* curves uniformed in terms of the range, the step width and the base axis. An interpolation-based method is applied to accomplish this.

When the *I–V* curves of all the units are ready, the operating point of each single unit from a given electrical bias (current, voltage or Ohmic load) of the module can be obtained, following an interpolation-based top–down tracing procedure that satisfies Kirchhoff's laws. When the tracking procedure reaches the cell level, each cell executes the procedure described in Fig. 3, the spatial information corresponding to the given module operating point is then

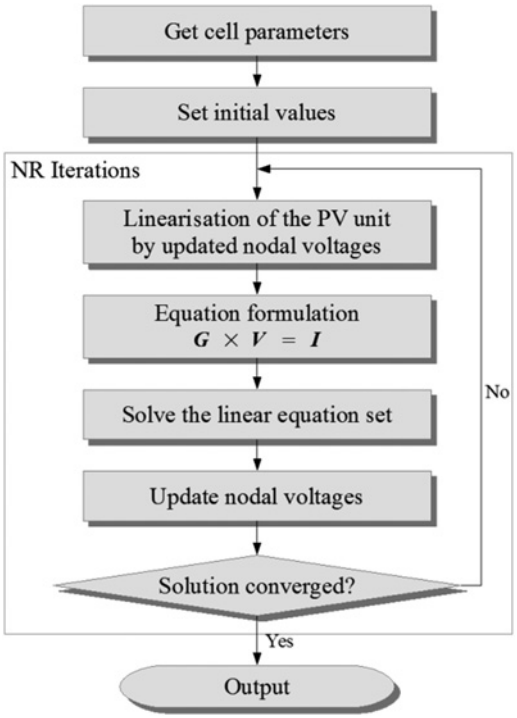

Fig. 4 *Flowchart shows the computational process for obtaining one operating point of a cell by NR iterations*

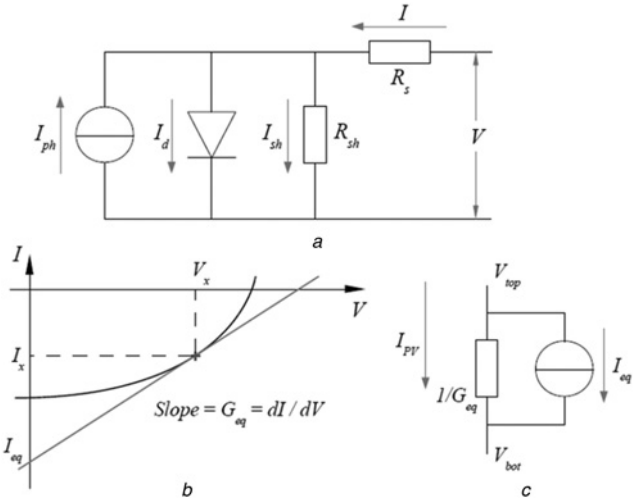

Fig. 5 *Linearisation of a one-diode PV model*

a Circuit diagram with reference directions marked

b Linearisation of the one-diode model according to a given operating voltage V_x

c Equivalent circuit of a one-diode model after linearisation

doi: 10.1049/iet-rpg.2013.0242

Table 1 Parameters of a-Si PV modules used in validation

irradiance (G)	1000 W/m^2
temperature (T)	25°C
photocurrent (I_{ph})	13.5 mA/cm^2
diode saturation Current (I_{sat})	1×10^{-7} mA/cm^2
series resistance (R_s)	11 Ω cm^2
shunt resistance (R_{sh})	530 kΩ cm^2
diode ideality factor (n)	2
front contact resistance (R_{front})	6 Ω/✓
back contact resistance (R_{back})	0.9 Ω/✓

calculated. Through this approach, the spatially non-uniform performance caused by the inhomogeneities of the module can be modelled.

3 Test results and discussions

To verify this modelling and simulation approach, some typical parameters of a-Si modules from the literature [8] are used, as shown in Table 1. a-Si technology is selected because in thin-film products the front contact layer has a relatively large area so that it is feasible to verify the influences of the lateral resistances. The same parameter set is used in two simulation tools for validation purposes. The first simulation tool for reference is PSpice. This is to verify the accuracy of the proposed NR solver. The other tool is a simulation program based on lumped modelling technique and I–V combination. This is to verify the validity of introducing lateral resistances. The normalised simulation results of a cell with a 10×10 sub-cell array are shown in Fig. 6.

PSpice is a mature and reliable circuit simulation tool based on SPICE (Simulation Program with Integrated Circuit Emphasis) that has been widely used as the simulation engine in modelling of PV devices [7–15, 17]. In PSpice simulation, the identical model structure and parameter set are utilised as such in the distributed network approach. Each I–V curve contains 200 data points. The comparison shows that the operating points calculated by the PV-oriented NR solver agree with those from PSpice. A small shifting can be read near V_{oc}. This can be because the different set up of the accuracy and the convergence criterion of the two solvers. Since numerical methods are used in solving the non-linear equation (5) and also the NR procedure, the deviations can be accumulated with the number of iterations, as well as round-off errors. The maximum shifting read from the data is 0.6%. It implies that in the NR solver with the PV-oriented linearisation process has an acceptable accuracy and is feasible for PV applications. The introduction of lateral resistances is required to understand the shape of the curves. Comparing with a conventional lumped resistance simulation, the one including lateral resistances results not only in non-uniform distribution of local operating points but also in additional overall apparent series resistances. It is noticeable that the fill factor is higher than that from the curve of the full network model in which lateral resistances take effect. For verification, the lateral resistances in the network model are then set to a very small value ($R_{lat} = 10^{-6}$ Ω/✓) to imitate a lumped case. It shows that the results from both tools have a good consistency as expected.

After the I–V characteristic of the module is obtained, if a global operating point is given, the corresponding operating point of each node can be calculated by the a top–down tracing process as described earlier. By applying the NR solver to each cell, the distributed nodal voltages can be produced and thus the current in each branch can be derived by Ohm's law. The distributed information is useful when there is non-uniformity in the module. An intuitive example is shown in Fig. 7. The EL result of an a-Si sample with the size 5 cm × 4 cm (Fig. 7*a*), with a forward biased current $I_{bias} = I_{sc}$, shows a noticeable gradient of signal strength along the width of the cell. The emission of infrared light is stronger near the positive terminal (on the

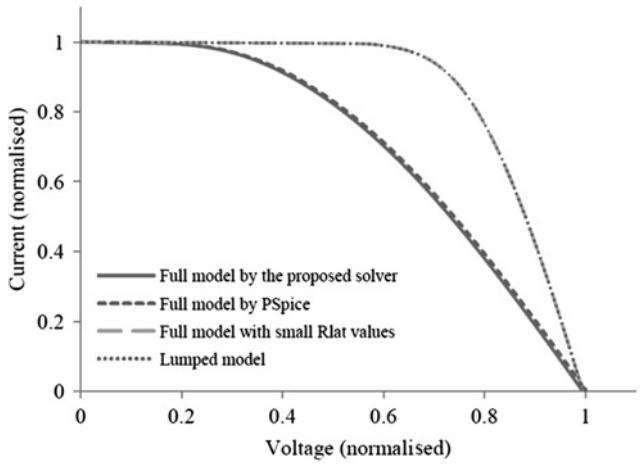

Fig. 6 *Verification of the distributed network modelling and simulation tool by PSpice and I–V combining*

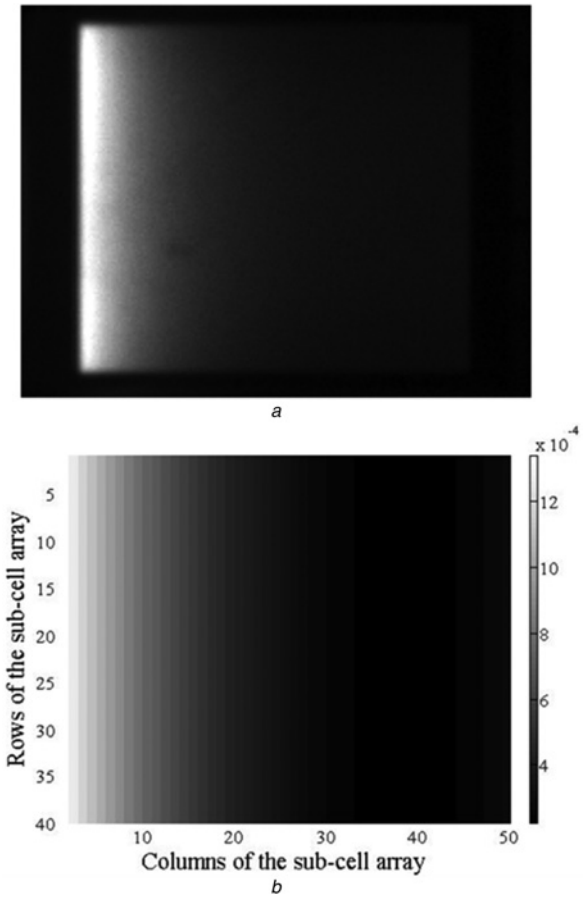

Fig. 7 *Distributed nodal voltages and the current in each branch*

a EL image of an a-Si cell with the size 5 cm (length) × 4 cm (width)
b Simulation result shows the relative value of local current absorption of the corresponding a-Si cell

doi: 10.1049/iet-rpg.2013.0242

left) because the lateral resistance accumulates along the width of the cell, which leads to a variation of electric potential and thus the local current absorption. A 40 (rows) × 50 (columns) sub-cell array, with the spatial resolution 1 mm × 1 mm, is used in a qualitative simulation. The intensity of EL signal is translated to the strength of local current absorption. The reproduced EL result is displayed with a grey scale where white represents the relative maximum current and black represents no current (Fig. 7*b*). The gradient pattern from the simulation successfully matches that of the EL image.

Spatially resolved characterisation techniques are powerful tools for detecting inhomogeneities in PV modules. Take EL, for example, it has been proven an effective characterisation

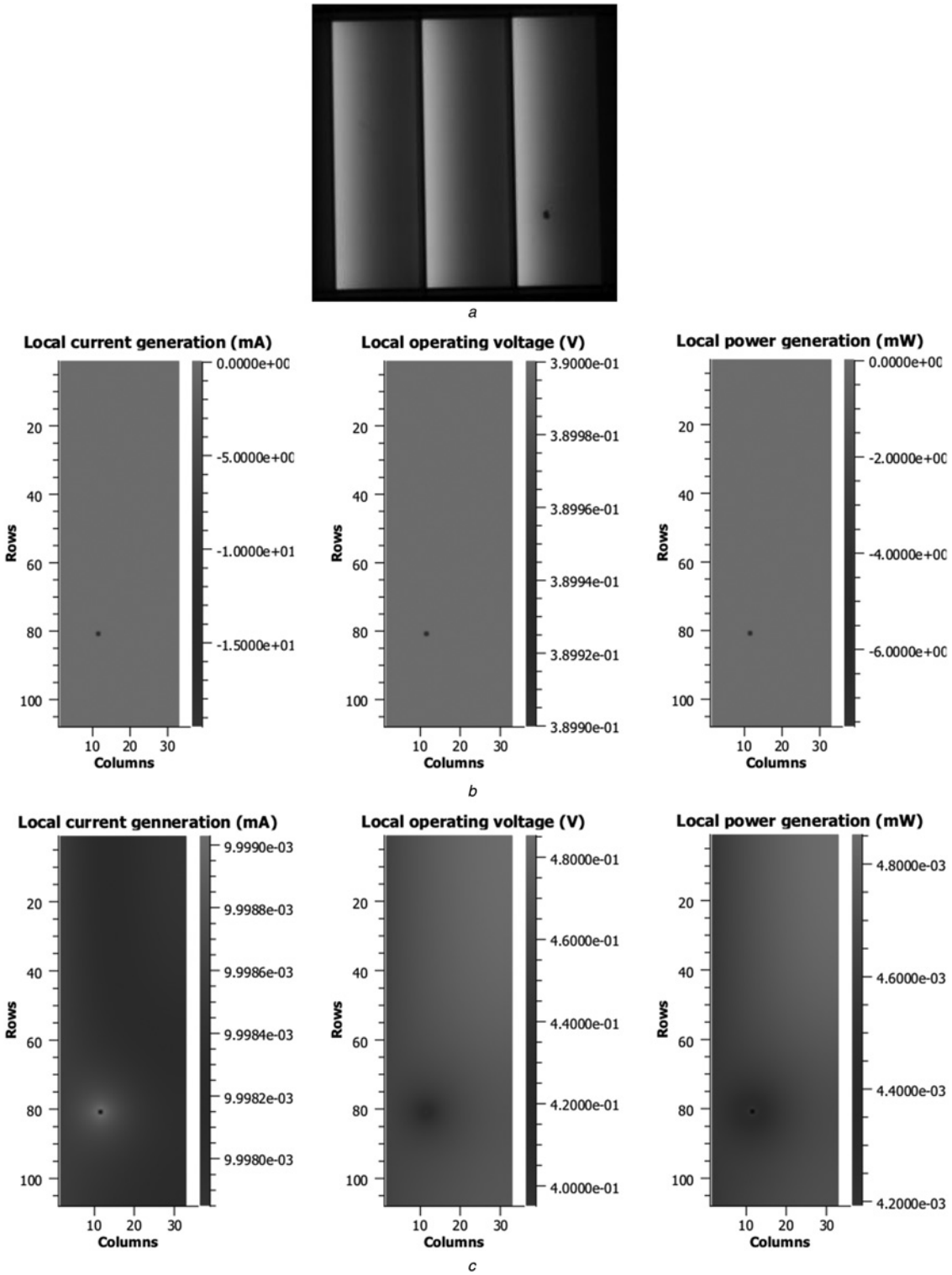

Fig. 8 *Modelling and simulation approach to predict local operating points of a module with a shunt detected by EL*

a EL measurement result of a three-cell a-Si module with a shunt on the third cell
b Simulation results of the third cell with no lateral resistance considered
c Simulation results of the third cell with lateral resistance included
All the results in (*b*) and (*c*) are obtained at MPP under STC

doi: 10.1049/iet-rpg.2013.0242

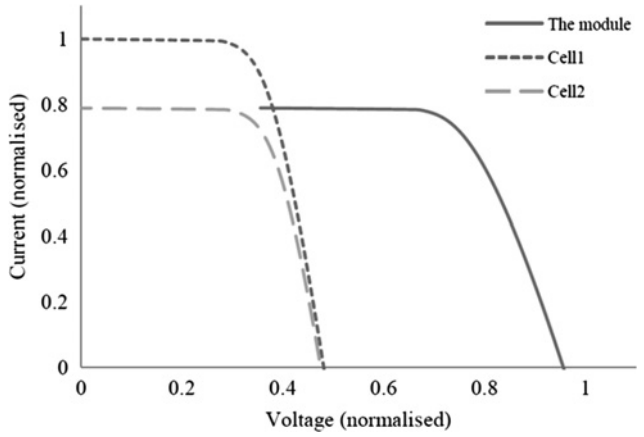

Fig. 9 *Mismatch effect caused by non-uniform irradiance in PV module with two identical cells in series*

tool for identifying shunts, series resistance, bandgap inhomogeneities etc. [17, 19–21]. In a production line, information of inhomogeneities can be used by the manufacturer for quality control. In real applications, the information can be used to predict the overall output of a module with defects. These implementations will require supports from modelling and simulation. Firstly, most spatially resolved characterisation techniques, especially imaging techniques, are naturally qualitative so that quantitative interpretations of experimental results have to be performed by a simulation tool. Secondly, for encapsulated modules, it is sometimes difficult to obtain the characteristics of individual components inside. Moreover, timing issue is considerable. It will be much more efficient to use a simulation when an experiment is relatively time-consuming.

Fig. 8 shows an example of using this modelling and simulation approach to predict the local operating points of a module with a shunt detected by EL. Local shunting is a common type of defects that can be detected in many PV devices. In EL images, by changing the path of the electrons from a radiative path to non-radiative, shunts usually become singular points and appear darker because current flows directly through them without emitting light from radiative recombination (Fig. 8*a*). In an operating PV device, a shunt can become a reverse-biased point in a cell and therefore reduce the output of the particular cell and thus the overall power generation. Figs. 8*b* and *c* show the simulation results as predictions of the local current generation of the cell with a shunt, under the standard test conditions (STC) and operating on the maximum power point (MPP), from a conventional *I–V* combination and the proposed distributed network approach, respectively. Each single cell is represented by a 108 (rows) × 36 (columns) sub-cell array with the resolution 0.5 mm × 0.5 mm. The shunt is introduced at the 80th row, 12th column in the third cell, according to the position read from the EL image, with the local parameters $R_{s(80,\ 12)} = 0.01\ \Omega$ and $R_{sh(80,\ 12)} = 0.01\ \Omega$. In the conventional modelling approach with no lateral resistance considered, the shunt is an independent reverse-biased point with no interference with the surrounding sub-cells. Thus, no variations of local operating points can be observed (Fig. 8*b*). The local operating current of the shunt point shows a negative value, that is, absorbing currents, indicating a reverse-biased point. This is also confirmed by the local power dissipation (the negative value) in the power map. The distributed modelling technique, on the other hand, is able to produce a non-uniform output (Fig. 8*c*). The reverse-biased operating point remains, but there are significant variations observed in the current, voltage and power maps. The variations are due to the existence of lateral resistances which create lateral current paths between nodes. Current intensity around the shunt is relatively high comparing the rest part in the whole cell, but the power generation in the same area is lower than the surroundings. The overall power generation as well as the fill factor are also reduced, which conforms to the expectation behaviour of a shunt in reality.

Fig. 9 demonstrates a simulation that investigating the mismatch effect caused by non-uniform irradiance. Non-uniform irradiance is an example of environmental inhomogeneities. It can be encountered in experiments with background illumination such as illuminated laser beam-induced current (LBIC). In LBIC, the background light is introduced to make the sample operate close to realistic operating conditions [8]. However, if the background illumination is non-uniform, it can cause considerable mismatch effects between cells in a multiple-cell module, which will lead to a misinterpretation of measurement results. For demonstration, a simulation for a two-cell module operating under non-uniform irradiance is set up. For simplicity, all electrical parameters are from Table 1. The local irradiance is set as 1000 W/m^2 for cell 1 and 800 W/m^2 for cell 2, representing a non-uniform background light. The simulation result suggests that firstly the non-uniform irradiance causes non-uniform current generation because the photocurrent in diode model is proportional to irradiance. Moreover, since cell 1 receives more light than cell 2, a variation on their *I–V* curves is observed. Since the two cells are connected in series in the module, the overall *I–V* curve of the module is limited by the characteristic of cell 2, according to KCL. The overall output of the module will be determined by the limited cell, that is, cell 2. In case of a laser scanning, a higher current value will be detected from cell 2 which is not necessarily the one with lower quality – the result is misinterpreted. To avoid this kind of misinterpretation, a limited LBIC approach was developed to eliminate the mismatch effect and to ensure the LBIC output reflect the real performance of the cell being scanned [8, 22].

Non-uniform module outputs caused by internal and external inhomogeneities have been studied. The simulations were carried out mainly qualitatively or semi-quantitatively. For a complete quantitative simulation that can fully reproduce spatially resolved characterisation results, a precise method that can identify the local electrical parameters of PV modules is still being investigated.

4 Conclusion

This paper presents a distributed electrical network modelling technique for PV modules. The proposed approach introduces a seven-level hierarchical architecture to describe a PV module in a spatially resolved manner and implements a PV-oriented nodal analysis method to obtain the local operating points. The approach has been verified by PSpice software. The case studies have shown that this modelling and simulation tool can be used to analyse spatially resolved characterisation results and to predict global and distributed operating points under different conditions.

doi: 10.1049/iet-rpg.2013.0242

More efforts on developing an effective parameter determination mechanism are needed so that a fully quantitative characterisation can be achieved by using the network modelling and simulation tool.

5 Acknowledgment

This work has been supported by a joint UK-India initiative in solar energy through a joint project 'Stability and Performance of Photovoltaics (STAPP)' funded by Research Councils UK (RCUK) Energy Programme in UK (contract no: EP/H040331/1) and by Department of Science and Technology (DST) in India.

6 References

1 Gottschalg, R., Rommel, M., Infield, D.G., Kearney, M.J.: 'Influence of the measurement environment on the accuracy of the extraction of the physical parameters of solar cells', *Meas. Sci. Technol.*, 1999, **10**, pp. 796–804
2 Gottschalg, R.: 'Environmental influences on the performance of thin film solar cells'. PhD thesis, Loughborough University, 2001
3 Quaschning, V., Hanitsch, R.: 'Numerical simulation of current-voltage characteristics of photovoltaic systems with shaded solar cells', *Sol. Energy*, 1996, **56**, (6), pp. 513–520
4 Villalva, M.G., Gazoli, J.R., Filho, E.R.: 'Comprehensive approach to modeling and simulation of photovoltaic arrays', *IEEE Trans. Power Electron.*, 2009, **24**, (5), pp. 1198–1208
5 Orozco-Gutierrez, M.L., Ramirez-Scarpetta, J.M., Spagnuolo, G., Ramos-Paja, C.A.: 'A technique for mismatched PV array simulation', *Renew. Energy*, 2013, **55**, pp. 417–427
6 Li, Y., Huang, W., Huang, H., *et al.*: 'Evaluation of methods to extract parameters from current–voltage characteristics of solar cells', *Sol. Energy*, 2013, **90**, pp. 51–57
7 Zekry, A., Al-Mazroo, A.Y.: 'A distributed SPICE-model of a solar cell', *IEEE Trans. Electron. Devices*, 1996, **43**, (5), pp. 691–700
8 Vorasayan, P.: 'Spatially resolved measurement of thin film silicon solar modules by laser beam induced current (LBIC) system'. PhD thesis, Loughborough University, 2010
9 Vorasayan, P., Betts, T.R., Gottschalg, R.: 'Spatially distributed model for the analysis of laser beam induced current (LBIC) measurements of thin film silicon solar modules', *Sol. Energy Mater. Sol. Cells*, 2011, **95**, (1), pp. 111–114
10 Monokroussos, C., Rüther, R., Gottschalg, R., Kong, M., Infield, D.G.: 'Effect of cell width on the device performance of amorphous silicon solar cells'. Proc. 17th European Photovoltaic Solar Energy Conf., Paris, France, June 2004, pp. 1489–1492
11 Galiana, B., Algora, C.: 'A 3-D model for concentrator solar cells based on distributed circuit units', *IEEE Trans. Electron. Devices*, 2005, **52**, (12), pp. 2552–2558
12 Breitenstein, O., Gupta, R., Schneider, J.: 'Surface potential mapping on crystalline silicon on glass solar modules', *J. Appl. Phys.*, 2007, **102**, (2), pp. 024511
13 Pieters, B.E.: 'Spatial modeling of thin-film solar modules using the network simulation method and SPICE', *IEEE J. Photovoltaics*, 2011, **1**, (1), pp. 93–98
14 Gupta, R., Somasundaran, P., Nandi, D.K.: 'Electrical simulation and characterization of shunts in solar cells', *Appl. Mech. Mater.*, 2011, **110–116**, pp. 2453–2457
15 Eidelloth, S., Haase, F., Brende, R.: 'Simulation tool for equivalent circuit modeling of photovoltaic devices', *IEEE J. Photovoltaics*, 2012, **99**, pp. 1–8
16 Bishop, J.W.: 'Computer simulation of the effects of electrical mismatches in photovoltaic cell interconnection circuits', *Sol. Cells*, 1988, **25**, pp. 73–89
17 Ott, T., Runai, F.R., Schwäble, F., Walter, T.: '2D network simulation and luminescence characterization of Cu(In, Ga)Se2 thin film modules', *Prog. Photovolt., Res. Appl.*, 2012, Special Issue: Adventures in Cu-Chalcogenide solar cells
18 Kielkowski, R.M.: 'Inside SPICE' (McGraw-Hill, 1998, 2nd edn.)
19 Fuyuki, T., Kitiyanan, A.: 'Photographic diagnosis of crystalline silicon solar cells utilizing electroluminescence', *Appl. Phys. A*, 2009, **96**, pp. 189–196
20 Trupke, T., Bardos, R.A., Abbott, M.D., *et al.*: 'Progress with luminescence imaging for the characterisation of silicon wafers and solar cells'. Proc. 22nd European Photovoltaic Solar Energy Conf., Munich, Germany, 2007, pp. 22–31
21 Kasemann, M., Grote, D., Walter, B., *et al.*: 'Luminescence imaging for the detection of shunts on silicon solar cells', *Prog. Photovolt., Res. Appl.*, 2008, **16**, pp. 297–305
22 Vorasayan, P., Betts, T.R., Gottschalg, R.: 'Limited laser beam induced current measurements: a tool for analysing integrated photovoltaic modules', *Meas. Sci. Technol.*, 2011, **22**, pp. 085702 (7pp)

doi: 10.1049/iet-rpg.2013.0242